



Selective zinc sensor based on pyrazoles and quinoline used to image cells



Hyun Kim^a, Ga Rim You^a, Gyeong Jin Park^a, Ji Young Choi^b, Insup Noh^b,
Youngmee Kim^c, Sung-Jin Kim^c, Cheal Kim^{a,*}, Roger G. Harrison^{d,*}

^a Department of Fine Chemistry and Department of Interdisciplinary Bio IT Materials, Seoul National University of Science & Technology, Seoul, 139-743 Republic of Korea

^b Department of Chemical Engineering, Seoul National University of Science & Technology, Seoul, 139-743 Republic of Korea

^c Department of Chemistry and Nano Science, Ewha Womans University, Seoul 120-750, Republic of Korea

^d Department of Chemistry and Biochemistry, Brigham Young University, Provo, UT, USA

ARTICLE INFO

Article history:

Received 12 July 2014

Received in revised form

6 October 2014

Accepted 7 October 2014

Available online 18 October 2014

Keywords:

Zinc sensor

Quinoline

Visible absorption

Cell imaging

Fluorescence

Selective

ABSTRACT

The synthesis, Zn²⁺ binding, crystal structure, and cell imaging studies of a new pyrazole amine quinoline receptor with a flexible binding pocket are described. Upon coordination to Zn²⁺, the absorption of the receptor increases at 364 nm and it fluoresces at 500 nm. The fluorescence response to Zn²⁺ is selective for Zn²⁺ and does not occur with other metal ions, not even Cd²⁺. In solution, the receptor forms 1:1 complexes with Zn²⁺, but in the solid-state two Zn²⁺ ions coordinate to the receptor. The aqueous solubility of the receptor allows for imaging of Zn²⁺ in living cells. Cells exposed to receptor and Zn²⁺ fluoresce when excited with visible light.

© 2014 Elsevier Ltd. All rights reserved.

1. Introduction

Zinc has a multitude of uses in organisms, including acting as a Lewis acid in hydrolytic enzymes, as a structure component of proteins, and as a signal in brain function. Due to the prevalence of Zn²⁺ in organisms, its detection and monitoring are essential to understand its role in biological organisms [1]. Without being colored or redox active it has been difficult to detect Zn²⁺ ions in biological environments. With its *d* orbitals full of electrons and those electrons stable, Zn²⁺ resembles Ca²⁺ more than other transition metal ions. Cellular levels of Zn²⁺ are not the same and thus different concentrations of cellular zinc need to be monitored. Therefore, receptors with high and low affinity for zinc are important [2]. However, no matter what the binding strength of the receptor is, selectivity for Zn²⁺ over other metal ions is critical.

The development of zinc sensors is an active research field. Most sensors have two components, a fluorophore and a Zn²⁺ binding site. Various molecules have been used as fluorophores, one of which has been quinoline [3]. We have developed receptors with

the amidoquinoline fluorophore due to the large enhanced fluorescence of quinoline after the amide binds to Zn²⁺ [4]. Several of the sensors are biocompatible and have been used to image cells [5].

The Zn²⁺ binding domain in sensors must chelate Zn²⁺ and thus often has several nitrogen atoms. Such ligands as dipicolylamine (DPA) have been employed as the chelates [6] and some cases they have been included with quinoline to make receptors [7]. A ligand that hasn't been used is the dipyrazolylamine. The dipyrazolylamine, with its pyrazole nitrogens separated from its amine nitrogen by three atoms, is able to form six-membered metal containing rings [8]. Metal ions such as Co²⁺, Ni²⁺, Cu²⁺ and Zn²⁺ have been coordinated to dipyrazolylamine ligands [9]. And in some cases the dipyrazolylamine ligand coordinates strongly to Zn²⁺ due to the flexible coordination of Zn²⁺, but less strongly to other transition metal ions, due to their preference to one definite geometry, such as octahedral geometry. The unique ability of Zn²⁺ to be a strong Lewis acid and yet to be stable in various geometric conformations renders it able to coordinate strongly to ligands to which other metal ions bind more weakly.

In this paper we present the synthesis and properties of a new zinc receptor that has a flexible binding site composed of pyrazoles. The receptor has an amidoquinoline unit as its fluorophore. The

* Corresponding authors.

E-mail addresses: chealkim@seoultech.ac (C. Kim), roger_harrison@byu.edu (R.G. Harrison).

new receptor fluoresces in the presence of Zn^{2+} , but not with other metal ions. A crystal structure of the receptor bonded to Zn^{2+} shows coordination to the Zn^{2+} through pyrazole nitrogens and the amide oxygen and nitrogen. The new receptor- Zn^{2+} complex has the important properties of being soluble in water and fluorescing when excited with visible light. The receptor is able to induce fluorescence in living cells that have been exposed to Zn^{2+} .

2. Results and discussion

2.1. Synthesis

The new receptor **1** was synthesized by adding 2-chloro-*N*-(quinolin-8-yl)acetamide to bis[2-(3,5-dimethylpyrazol-1-yl)ethyl]-amine in the presence of base (Scheme 1). Column chromatography was used to isolate pure product, which showed methylene proton NMR signals next to the carbonyl group to be at 3.4 ppm, signifying receptor assembly. The molecule is colorless and does not fluoresce.

2.2. Fluorescence due to Zn^{2+}

Upon addition of Zn^{2+} to an aqueous solution of receptor, the receptor fluoresces. The fluorescence at 500 nm increases upon excitation at 356 nm until one equivalent of Zn^{2+} has been added (Fig. 1). Importantly, the fluorescence response is selective for Zn^{2+} and the sensor doesn't fluoresce when other metal ions such as Na^+ , K^+ , Mg^{2+} , Ca^{2+} , Al^{3+} , Cr^{3+} , Mn^{2+} , Fe^{2+} , Fe^{3+} , Co^{2+} , Ni^{2+} , Cu^{2+} , Cd^{2+} , Pb^{2+} , Ga^{3+} , and In^{3+} are present (Fig. 2). Remarkably, unlike many other Zn^{2+} sensors, the receptor does not fluoresce in the presence of Cd^{2+} . Not only is the receptor selective for Zn^{2+} , but other metal ions do not quench the fluorescence caused by Zn^{2+} . The fluorescence of the Zn-receptor complex is not affected when one equivalent of metal ion, such as Na^+ , K^+ , Mg^{2+} , Ca^{2+} , Al^{3+} , Cr^{3+} , Mn^{2+} , Fe^{2+} , Fe^{3+} , Co^{2+} , Ni^{2+} , Cu^{2+} , Cd^{2+} , Pb^{2+} , Ga^{3+} , and In^{3+} is present (Fig. 3). Larger equivalents (2, 5, and 10 equivalents) of Cr^{3+} , Fe^{3+} , Co^{2+} , and Cu^{2+} do reduce the fluorescence intensity of the Zn-receptor complex, however, it still remains over fifty percent of its original value.

2.3. pH range of fluorescence

Fluorescing at biologically relevant pH is important for the usefulness of the receptor. The fluorescence enhancement of the receptor caused by Zn^{2+} is maintained over a pH range from 6 to 11 (Fig. 4). The continuous fluorescence over five pH units implies that the Zn-receptor complex is stable over this pH range.

2.4. Fluorescence cycling

The receptor also shows chelation ability over several binding episodes. The fluorescence of the Zn-receptor complex is quenched when EDTA is added to it, but when more Zn^{2+} is added to the solution, the fluorescence returns (Fig. 5). This fluorescence

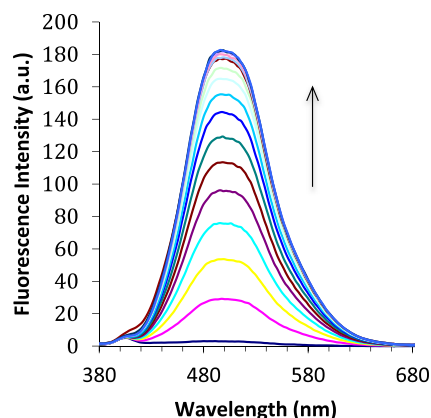


Fig. 1. Fluorescence intensity increase due to Zn^{2+} addition to receptor **1**. Conditions: 10 μM receptor in bis-tris aqueous solution, 356 nm excitation, 0 to 2 equivalents of Zn^{2+} added in 0.1 equiv. portions.

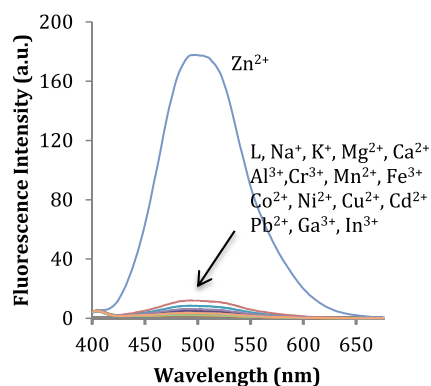
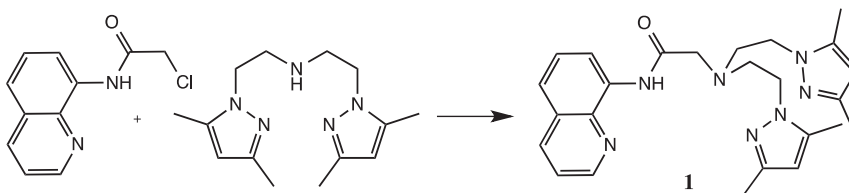


Fig. 2. Receptor fluorescence due to Zn^{2+} . Other metal ions do not cause fluorescence. Conditions: 10 μM receptor in bis-tris aqueous solution, 356 nm excitation, 1 equiv. metal nitrate.

quenching and emission can be cycled several times without loss of fluorescence intensity. The binding constant of EDTA to Zn^{2+} is of the order of 10^{16} M^{-1} and is much larger than the $1.1 \times 10^7 \text{ M}^{-1}$ binding constant for receptor to Zn^{2+} . Thus EDTA removes Zn^{2+} from the Zn-receptor complex. With this binding constant for the receptor- Zn^{2+} complex and the strong fluorescence intensity of the complex, the detection limit of Zn^{2+} by the receptor is 30 nM.

2.5. Absorption change upon Zn^{2+} binding

The receptor has absorption bands at 220 and 325 nm. Both of these bands decrease in intensity when Zn^{2+} is added and new bands at 274 nm ($\epsilon = 2.4 \times 10^4 \text{ M}^{-1}\text{cm}^{-1}$) and 364 nm ($\epsilon = 3.7 \times 10^3 \text{ M}^{-1}\text{cm}^{-1}$) develop (Fig. 6). This red shift in the amide and aromatic π to π^* transitions upon Zn^{2+} binding has been noted before with quinoline receptors. We attribute it to a greater lowering



Scheme 1. Synthesis of receptor **1**. Conditions: reflux in acetonitrile with triethylamine.

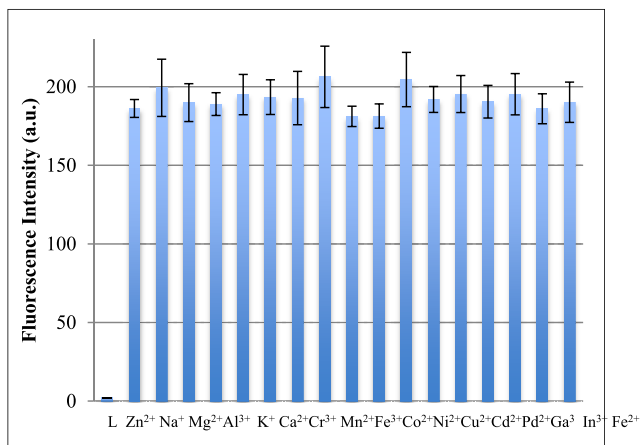


Fig. 3. Fluorescence of Zn-receptor complex remains in the presence of other metal ions. Conditions: 10 μM receptor in bis-tris aqueous solution, 356 nm excitation, 1 equiv. of Zn^{2+} and other metal ion.

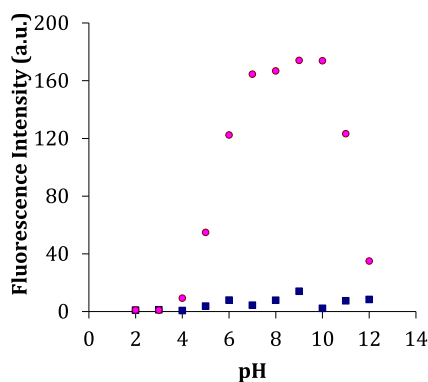


Fig. 4. The receptor in the presence of Zn^{2+} fluoresces from pH 6 to 11. The receptor without Zn^{2+} does not fluoresce at any pH. Conditions: 10 μM receptor in bis-tris aqueous solution, 356 nm excitation, 1 equiv. metal nitrate.

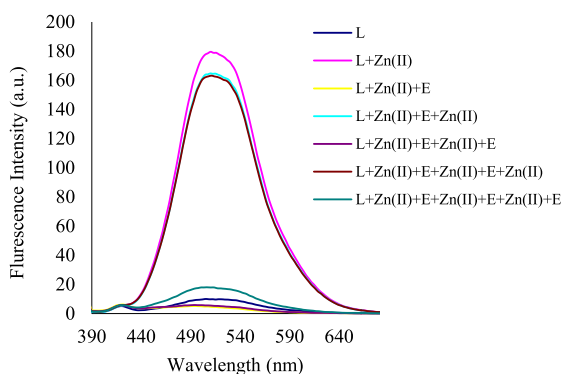


Fig. 5. EDTA eliminates the fluorescence of the Zn^{2+} -receptor complex. Receptor (10 μM) with 1 eq of Zn^{2+} fluoresces. When 1 eq of EDTA is added to this solution, the fluorescence is quenched. Adding more Zn^{2+} reestablishes the fluorescence. (L = receptor, E = EDTA.)

of the π^* orbitals than the lowering of the π orbitals. The nitrogen in the quinoline is important to this absorption shift and this shift implies binding of the Zn^{2+} to the nitrogen in the quinoline [4c].

2.6. NMR characterization of **1**

The ^1H NMR signals of the receptor change upon Zn^{2+} binding. In aqueous solution there is a large downfield shift (nearly

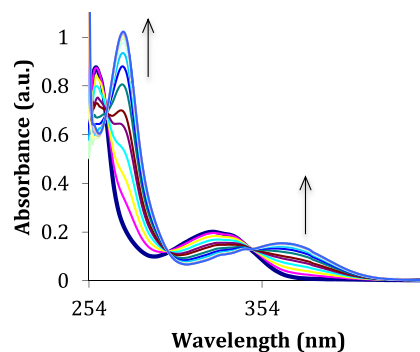


Fig. 6. Receptor absorption changes due to Zn^{2+} . Peaks at 274 and 364 nm grow in as Zn^{2+} is added. Conditions: 40 μM receptor in bis-tris aqueous solution, Zn^{2+} added by 0.1 equiv.

0.75 ppm) of the proton signal from the hydrogen on the pyrazole ring, which is complete after one equivalent of Zn^{2+} (SI Fig. s1). This downfield movement is attributed to coordination of electropositive Zn^{2+} , which results in the pyrazole hydrogens being more deshielded. The three aromatic proton signals of the quinoline divide into six, indicating multiple environments for quinolines, which remain even when two equivalents of Zn^{2+} have been added. The receptor hydrogens being in multiple environments upon Zn^{2+} binding is also displayed by the methylene protons of the ethyl groups, which give rise to several signals. In acetonitrile, the receptor has a less complicated spectrum and gives only one signal for each hydrogen. As in aqueous media, the proton signal of the pyrazole moves downfield (0.5 ppm) upon Zn^{2+} coordination (SI Fig. 2). In a similar manner, the methylene proton signals all move downfield. The aromatic proton signals, however, stay in the region 7.5–9.0 ppm. The NH proton signal moves upfield by nearly 0.5 ppm, indicating Zn^{2+} coordination.

The ^1H NMR, fluorescence and absorption spectra support 1:1 binding of receptor to Zn^{2+} , since the hydrogen, emission, and absorption peaks stop changing after one equivalent of Zn^{2+} has been added. Also, in aqueous and dilute methanol solutions, Job plots show a 1:1 binding ratio of Zn^{2+} to receptor (SI Fig. 3). Mass spectra also support the 1:1 Zn^{2+} to receptor coordination. The base peak (100% relative abundance) indicates a mass of 508.27 m/z , which corresponds to receptor + Zn^{2+} - H^+ .

2.7. Crystal structure analysis

To further understand the Zn^{2+} coordination to receptor **1**, crystals of the Zn^{2+} -receptor complex were grown. Single crystals of the receptor bound to Zn^{2+} showed two zinc ions coordinated to one receptor (Fig. 7). Both zinc ions had distorted octahedral geometry. One Zn^{2+} was bound to the nitrogens of the amine and pyrazoles, and to oxygens from the amide and a nitrate. The other Zn^{2+} was bound to the nitrogens of the quinoline and amide and to oxygens of two nitrates. The Zn–N bond lengths are from 2.0 to 2.2 Å, except for the Zn–N amide bond length, which is shorter and 1.85 Å. The Zn–O amide bond length is 2.11 Å, similar to the Zn–O bonds of one of the nitrate ions. The C–O bond length of the amide is 1.20 Å and similar in length to a C–O double bond. The C–N amide bond length of 1.36 Å is also short and less than a typical C–N single bond, but similar to a C–N bond in an amide. As shown by the crystal structure, the receptor can bind two Zn^{2+} ions. Although this 1:2 receptor to Zn^{2+} ratio is different than what was observed in solution, it was also observed in concentrated methanolic solutions, where a Job plot shows a 1:2 ratio of receptor to Zn. It seems that when Zn^{2+} concentrations are high, the receptor binds two Zn^{2+} ions.

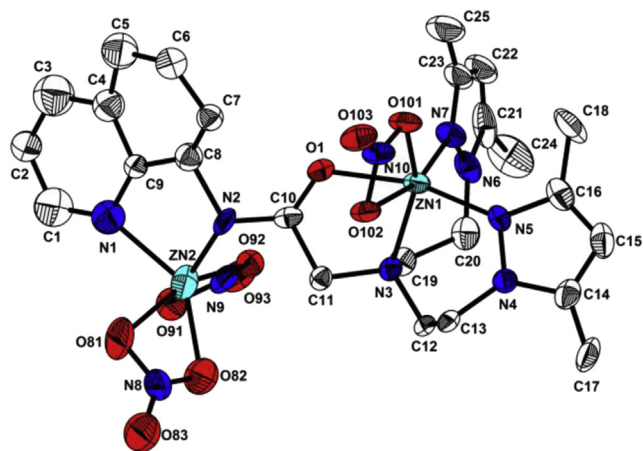


Fig. 7. Crystal structure of Zn-receptor complex. Atom color: C grey, O red, N blue, and Zn light blue. Hydrogens were omitted for clarity. (For interpretation of the references to colour in this figure legend, the reader is referred to the web version of this article.)

2.8. Cell studies

Given the strong fluorescence response by the receptor to Zn^{2+} we investigated the particle application of the receptor and the detection of Zn^{2+} in living cells. Human dermal fibroblast cells exposed to 30 μM receptor and 100 and 150 μM $Zn(NO_3)_2$ fluoresced, while those exposed to 0 and 50 μM $Zn(NO_3)_2$ did not (Fig. 8). When the cells were exposed to Zn^{2+} and greater concentrations of receptor, such as 50, 100, and 150 μM , even 50 μM Zn^{2+} cells fluoresced. Zn^{2+} was found throughout the cell, as shown by fluorescence everywhere in the cell.

3. Conclusion

A new Zn^{2+} receptor composed of pyrazoles and 4-aminoquinoline has been synthesized. The receptor binds to two Zn^{2+} ions shows bonding through all of the receptor nitrogens in the crystal structure. The receptor fluoresces in the presences of small quantities of Zn^{2+} , but not with other metal ions. Also, the receptor- Zn^{2+} complex maintains fluorescence in the presence of other metal ions such as Cd^{2+} , Cu^{2+} , Ni^{2+} , Co^{2+} , and Fe^{2+} . With the binding of Zn^{2+} comes a change to the 1H NMR signals of the

receptor. As Zn^{2+} binds to the receptor, its absorption at 364 nm increases and tails off into the visible light region, which allows for receptor excitation with visible light. The receptor- Zn^{2+} complex is soluble in aqueous solutions and results in fluorescence of living cells that are exposed to receptor and Zn^{2+} .

4. Experimental section

4.1. Materials and instrumentation

All the solvents and reagents (analytical and spectroscopic grade) were obtained from Sigma Aldrich and used as received. NMR spectra were recorded using a Varian 400 spectrometer. Chemical shifts (δ) were reported in ppm, relative to tetramethylsilane ($Si(CH_3)_4$). Absorption spectra were recorded at 25 $^\circ C$ using a Perkin Elmer model Lambda 2S UV/Vis spectrometer. Electrospray ionization mass spectra (ESI-MS) were collected using a Thermo Finnigan (San Jose, CA, USA) LCQTM Advantage MAX quadrupole ion trap instrument. Fluorescence measurements were performed using a Perkin Elmer model LS45 fluorescence spectrometer. 2-Chloro-*N*-(quinolin-8-yl)-acetamide [10] and bis[2-(3,5-dimethylpyrazol-1-yl)ethyl]-amine [11] were prepared according to procedures reported in the literature.

4.2. Synthesis of receptor 1 (2-(bis(2-(3,5-dimethyl-1H-pyrazol-1-yl)ethyl)amino)-*N*-(quinolin-8-yl)acetamide)

2-Chloro-*N*-(quinolin-8-yl)acetamide (0.46 g, 2.1 mmol), bis[2-(3,5-dimethylpyrazol-1-yl)ethyl]-amine (0.52 g, 2.0 mmol) and triethylamine (0.31 mL, 2.2 mmol) were dissolved in acetonitrile (30 mL), stirred and refluxed for 1 day under a nitrogen atmosphere. The solution was extracted with dichloromethane, the organic phase was separated, and the solvent was removed under vacuum. The pure product was obtained by column chromatography (silica gel, chloroform–methanol (10/1, v/v)). Yield: 0.24 g (55%). 1H NMR (400 MHz, $DMSO-d_6$, 25 $^\circ C$): δ = 10.92 (s, 1H), 8.86 (d, J = 3.6 Hz, 1H), 8.64 (d, J = 8 Hz, 1H), 8.40 (d, J = 8 Hz, 1H), 7.58 (m, 3H), 5.64 (s, 1H), 4.08 (t, J = 6.6 Hz, 4H), 3.38 (s, 2H), 2.95 (t, J = 6.6 Hz, 4H), 2.10 (s, 6H), 1.95 (s, 6H) ppm. ^{13}C NMR (400 MHz, $CDCl_3$, 25 $^\circ C$): δ = 169.7, 158.1, 157.3, 148.7, 148.5, 139.1, 137.6, 136.3, 134.5, 131.5, 129.9, 128.2, 127.5, 123.6, 122.9, 122.2, 121.9, 119.3, 117.5, 117.1, 59.1, 58.5, 56.5 ppm. HRMS (ESI): m/z calcd for $C_{24}H_{22}N_4O_2 + H^+$: 399.17; found 399.07. Elemental analysis calcd

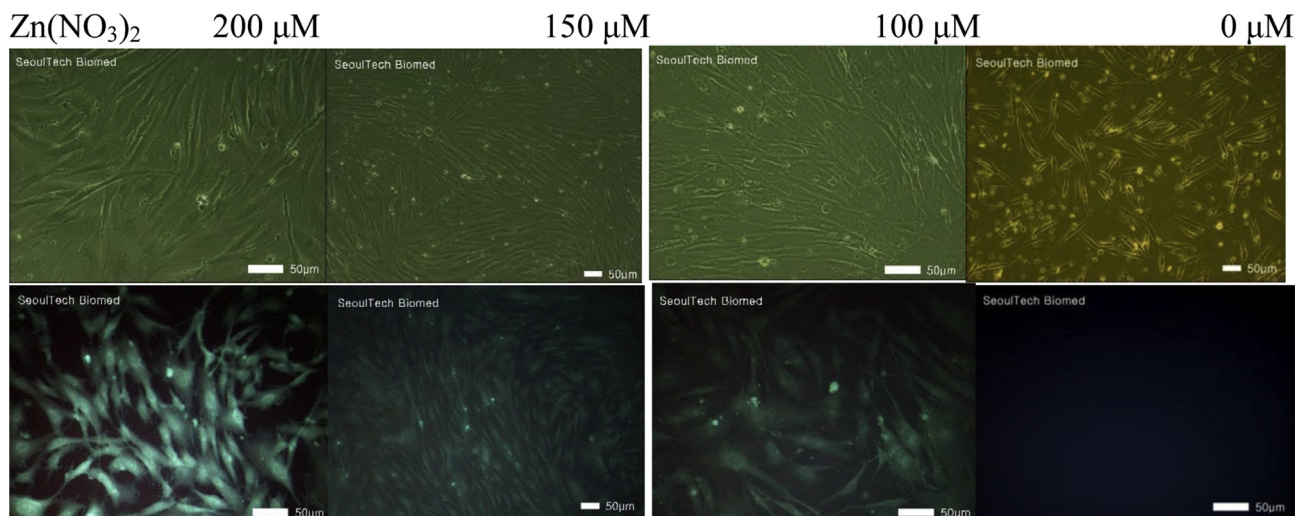


Fig. 8. Human dermal fibroblast cells exposed to different Zn^{2+} concentrations and 30 μM receptor. The pictures were taken with a light microscope (top) and fluorescent microscope (bottom).

(%) for $C_{24}H_{22}N_4O_2$ (398.46): C, 72.34; H, 5.57; N, 14.06; found: C, 72.15; H, 4.95; N, 13.75.

4.3. Fluorescence titration of Zn^{2+} with receptor

Receptor **1** (1.33 mg, 0.003 mmol) was dissolved in methanol (1 mL) and 10 μ L of the receptor solution (3 mM) was diluted with 2.990 mL bis-tris buffer solution (pH 7.1) to make a final concentration of 10 μ M. $Zn(NO_3)_2 \cdot 6H_2O$ (12.14 mg, 0.04 mmol) was dissolved in bis-tris buffer (4 mL). 0.3–3 μ L of the Zn^{2+} solution (10 mM) were transferred to the receptor solution (10 μ M). After mixing for a few seconds, fluorescence spectra after excitation at 365 nm were taken at room temperature.

4.4. UV–vis titration of Zn^{2+} with receptor

Receptor **1** (1.33 mg, 0.003 mmol) was dissolved in methanol (1 mL) and 40 μ L of the receptor solution (3 mM) were diluted with 2.960 mL bis-tris buffer solution to make a final concentration of 40 μ M. $Zn(NO_3)_2 \cdot 6H_2O$ (12.14 mg, 0.04 mmol) was dissolved in bis-tris buffer (4 mL). 1.2–12 μ L of the Zn^{2+} solution (10 mM) were transferred to the receptor solution (40 μ M). After mixing for a few seconds, fluorescence spectra were taken at room temperature.

4.5. Competitive metal ion experiments

Receptor **1** (1.33 mg, 0.003 mmol) was dissolved in methanol (1 mL) and 10 μ L of receptor solution (3 mM) were diluted with 2.990 mL bis-tris buffer solution to make a final concentration of 10 μ M. $M(NO_3)_2$ ($M = Na, K, 0.04$ mmol), $M(NO_3)_2$ ($M = Mn, Ni, Cu, Zn, Cd, Mg, Ca, Pb, 0.04$ mmol), or $M(NO_3)_3$ ($M = Al, Fe, Cr, 0.04$ mmol) were separately dissolved in bis-tris buffer (4 mL). 3 μ L of each metal solution (10 mM) were taken and added to 3 mL of each receptor solution (10 μ M) prepared as above to make a 1 equiv. metal ion solution. Then, 3 μ L of $Zn(NO_3)_2$ solution (10 mM) were added to the mixed solution of each metal ion and receptor to make a 1 equiv. Zn^{2+} solution. After mixing for a few seconds, fluorescence spectra were taken at room temperature.

4.6. Job plot measurement of Zn^{2+} with receptor

Receptor **1** (2.22 mg, 0.005 mmol) was dissolved in methanol (1 mL). 40, 36, 32, 28, 24, 20, 16, 12, 8, and 4 μ L of the receptor solution were taken and transferred to vials. Each vial was diluted with buffer solution to make a total volume of 4.960 mL. $Zn(NO_3)_2 \cdot 6H_2O$ (12.14 mg, 0.04 mmol) was dissolved in bis-tris (4 mL). 0, 4, 8, 12, 16, 20, 24, 28, 32, 36, and 40 μ L of the $Zn(NO_3)_2$ solution were added to each diluted receptor **1** solution. Each vial had a total volume of 5.00 mL. After shaking the solutions for a few minutes, fluorescence spectra were taken at room temperature.

4.7. NMR titration of Zn^{2+} with receptor

Four NMR tubes of **1** (4.45 mg, 0.01 mmol) dissolved in CD_3OD-D_2O (1/1, v/v, 0.5 mL) were prepared and four different equivalents (0, 0.5, 1 and 2 equiv.) of $Zn(NO_3)_2$ dissolved in CD_3OD-D_2O (1/1, v/v, 0.5 mL) were added separately to the receptor solutions. After shaking the solutions for a few seconds, the 1H NMR spectra were taken.

4.8. EDTA reversibility of receptor

Receptor **1** (1.33 mg, 0.003 mmol) was dissolved in methanol (1.0 mL) and 10 μ L of receptor solution (3 mM) were diluted with 2.990 mL of bis-tris buffer solution to make a final concentration of

10 μ M. $Zn(NO_3)_2$ (0.04 mmol) was dissolved in bis-tris buffer (4.0 mL). Three μ L of the Zn^{2+} solution (10 mM) were added to 3.0 mL of each receptor solution (10 μ M) to make 1 equiv. After mixing for a few seconds, a fluorescence spectrum was taken of the solution at room temperature. Ethylenediaminetetraacetic acid disodium salt dihydrate (EDTA, 0.050 mmol) was dissolved in bis-tris buffer (5 mL) and 3 μ L of the EDTA solution (10 mM) were added to the receptor- Zn^{2+} solution (10 μ M) prepared earlier. After mixing for a few seconds, a fluorescence spectrum of the solution was taken. For the reversibility study, another 3 μ L of the Zn^{2+} ion solution (10 mM) was added to the above solution. After mixing it for few seconds, the fluorescence spectra were taken at room temperature. The same experimental procedure was repeated two more times.

4.9. X-ray data collection and structural determination

$Zn(NO_3)_2$ (0.030 g, 0.10 mmol) was added to a stirred solution of receptor **1** (0.040 g, 0.090 mmol) in methanol (3 mL), and carefully layered with diethyl ether (5 mL). Colorless crystals suitable for X-ray analysis were obtained in a week. A colorless triclinic-type crystal, approximate dimensions of 0.16 mm \times 0.14 mm \times 0.12 mm, was used for X-ray crystallographic analysis. The diffraction data were collected on a Bruker SMART APEX diffractometer equipped with a monochromator using the Mo $K\alpha$ ($k = 0.71073$ Å) incident beam. The crystal was mounted on a glass fiber. The CCD data were integrated and scaled using the BRUKER-SMART software package, and the structure was solved and refined using SHELXL V6.12. All hydrogen atoms, except the amide hydrogen atom were located in the calculated positions. Selected bond lengths and angles are listed in Table 1. Structural information was deposited at the Cambridge Crystallographic Data Center (CCDC 972999).

Crystallographic data for **1**- $Zn(NO_3)_2$: $C_{25}H_{24}N_{10}O_{10}Zn_2$, $M = 755.28$, triclinic, space group P-1, $a = 9.7270(19)$ Å, $b = 12.859(3)$ Å, $c = 13.628(3)$ Å, $\alpha = 107.31(3)^\circ$, $\beta = 93.51(3)^\circ$, $\gamma = 90.04(3)^\circ$, $V = 1624.0(6)$ Å³, room temperature, $Z = 2$, $\mu = 1.545$ mm⁻¹, $\rho_c = 1.545$ g/cm³, crystal size 0.16 \times 0.14 \times 0.12 mm³, 8869 reflections collected with 6005 being independent ($R_{int} = 0.0337$); the final R_I and $wR(F^2)$ values were 0.1202 [$I > 2\sigma(I)$] and 0.3415, respectively; data completeness to $\theta = 26.00^\circ$ 97.3%; goodness-of-fit on $F^2 = 1.344$.

4.10. Cell imaging

Normal human primary dermal fibroblast cells in low passage (passage 6) were cultured in FGM-2 medium (Lonza, Switzerland) supplemented with 10% fetal bovine serum and 1% penicillin/streptomycin in an in vitro incubator with 5% CO₂ at 37 °C. Cells were seeded onto a 8 well plate (SPL Lifesciences, Korea) at a density of 2×10^5 cells per well and then incubated at 37 °C for 4 h after addition of various concentrations (0–150 μ M) of $Zn(NO_3)_2$. After washing two times with phosphate buffered saline (PBS) to

Table 1
Selected bond lengths (Å) and angles (°) for the Zn receptor complex.

Zn(1)–O(1)	2.108 (6)	Zn(2)–N(1)	2.147 (5)
Zn(1)–O(101)	1.984 (6)	Zn(2)–N(2)	1.853 (9)
Zn(1)–N(3)	2.024 (7)	Zn(2)–O(82)	2.109 (10)
Zn(1)–N(5)	2.095 (7)	Zn(2)–O(92)	2.122 (2)
Zn(1)–N(7)	2.225 (8)	Zn(2)–O(81)	2.387 (12)
C(10)–O(1)	1.200 (10)	Zn(2)–O(91)	2.420 (15)
N(3)–Zn(1)–O(1)	75.2 (3)	N(2)–Zn(2)–N(1)	90.80 (18)
O(1)–Zn(1)–N(7)	90.1 (3)	N(1)–Zn(2)–O(81)	91.9 (3)
N(3)–Zn(1)–N(5)	94.7 (3)	N(2)–Zn(2)–O(81)	102.2 (4)
N(5)–Zn(1)–N(7)	106.0 (3)	N(1)–Zn(2)–O(91)	79.8 (4)
O(101)–Zn(1)–N(5)	88.7 (3)	N(2)–Zn(2)–O(91)	136.7 (4)
O(101)–Zn(1)–O(1)	91.6 (3)	O(81)–Zn(2)–O(91)	120.2 (4)

remove the remaining $\text{Zn}(\text{NO}_3)_2$, the cells were incubated with receptor **1** (30 μM) at room temperature for 30 min. The cells were observed using a microscope (Olympus, Japan). The fluorescent images of the cells were obtained using a fluorescence microscope (Leica DMLB, Germany) at the excitation wavelength of 425 nm.

Acknowledgments

Financial support from Converging Research Center Program through the National Research Foundation of Korea (NRF) funded by the Ministry of Education, Science and Technology (2012001725 and 2012008875), and Brigham Young University is gratefully acknowledged.

Appendix A. Supplementary data

Supplementary data related to this article can be found at <http://dx.doi.org/10.1016/j.dyepig.2014.10.006>.

References

- Lim NC, Freake HC, Brückner C. Illuminating zinc in biological systems. *Chem Eur J* 2005;11:38–49;
 - Dai Z, Canary JW. Tailoring tripodal ligands for zinc sensing. *New J Chem* 2007;31:1708–18;
 - Que EL, Eomaille W, Chang CJ. Metals in neurobiology: probing their chemistry and biology with molecular imaging. *Chem Rev* 2008;108:1517–49;
 - Tomat E, Lippard SJ. Imaging mobile zinc in biology. *Curr Opin Chem Biol* 2010;14:225–30.
- McQuade LE, Lippard SJ. Cell-trappable quinoline-derivatized fluoresceins for selective and reversible biological Zn(II) detection. *Inorg Chem* 2010;49:9535–45;
 - Smith BA, Akers WJ, Leevy WM, Lampkins AJ, Xiao S, Wolter W, et al. Optical imaging of mammary and prostate tumors in living animals using a synthetic near infrared zinc(II)-dipolyamine probe for anionic cell surfaces. *J Am Chem Soc* 2010;132:67–9;
 - Xu Z, Baek KH, Kim HN, Cui J, Qian X, Spring DR, et al. Zn^{2+} -triggered amide tautomerization produces a highly Zn^{2+} -selective, cell-permeable, and ratiometric fluorescent sensor. *J Am Chem Soc* 2010;132:601–10;
 - Nolan EM, Lippard SJ. Small-molecule fluorescent sensors for investigating zinc metalloneurochemistry. *Acc Chem Res* 2009;42:193–203;
 - Mei Y, Frederickson CJ, Giblin LJ, Weiss JH, Medvedeva Y, Bentley PA. Sensitive and selective detection of zinc ions in neuronal vesicles using PYDPY1, a simple turn-on dipyrin. *Chem Commun* 2011;47:7107–9.
- Zhang Y, Guo X, Jia L, Zu S, Xu Z, Zheng L, et al. Substituent-dependent fluorescent sensors for zinc ions based on carboxamidoquinoline. *Dalton Trans* 2012;41:11776–82;
 - Zhang Y, Guo X, Si W, Jia L, Qian X. Ratiometric and water-soluble fluorescent zinc sensor of carboxamidoquinoline with an alkoxyethylamino chain as receptor. *Org Lett* 2008;10:473–6;
 - Zhou X, Yu B, Guo Y, Tang X, Zhang H, Liu W. Both visual and fluorescent sensor for Zn^{2+} based on quinoline platform. *Inorg Chem* 2010;49:4002;
 - Zhou X, Li P, Shi Z, Tang X, Chen C, Liu W. A highly selective fluorescent sensor for distinguishing cadmium from zinc ions based on a quinoline platform. *Inorg Chem* 2012;51:9226–31;
 - Wang RM, Huang SB, Zhao N, Chen ZN. A new Zn^{2+} chemosensor based on functionalized 8-hydroxyquinoline. *Inorg Chem Commun* 2010;13:1432–4;
 - Núñez C, Bastida R, Macías A, Bértolo E, Fernandes L, Capelo JL, et al. Synthesis, characterization, and fluorescence behavior of four novel macrocyclic emissive ligands containing a flexible 8-hydroxyquinoline unit. *Tetrahedron* 2009;65:6179–88;
 - Mameli M, Aragoni MC, Arca M, Atzori M, Bencini A, Bazzicalupi C, et al. Synthesis and coordination properties of quinoline pendant arm derivatives of [9]aneN₃ and [9]aneN₂S as fluorescent zinc sensors. *Inorg Chem* 2009;48:9236–49;
 - Jiang J, Xiaoliang T, Yang L, Dou W, Liu W, Fang R, et al. An efficient sensor for Zn^{2+} and Cd^{2+} based on different binding modes. *Dalton Trans* 2011;40:6367–70;
 - Ravikumar I, Ghosh P. Zinc(II) and PPI selective fluorescence off-on-off functionality as a chemosensor in physiological conditions. *Inorg Chem* 2011;50:4229–31;
 - Zhao C, Zhang Y, Feng P, Cao J. Development of a borondipyrromethane-based Zn^{2+} fluorescent probe: solvent effects on modulation sensing ability. *Dalton Trans* 2012;41:831;
 - Zhu JF, Yuan H, Chan WH, Lee AWM. A FRET fluorescent chemosensor SPAQ for Zn^{2+} based on a dyad bearing spiropyran and 8-aminoquinoline unit. *Tetrahedron Lett* 2010;51:3550–4.
- Song EJ, Kang J, You GR, Park GJ, Kim Y, Kim SJ, et al. A single molecule that acts as a fluorescence sensor for zinc and cadmium and colorimetric sensor for cobalt. *Dalton Trans* 2013;42:15514;
 - Kim JH, Hwang IH, Jang SP, Kang J, Kim S, Noh I, et al. Zinc sensors with lower binding affinities for cellular imaging. *Dalton Trans* 2013;42:5500–7;
 - Lee HG, Lee JH, Jang SP, Hwang IH, Kim SJ, Kim Y, et al. Zinc selective chemosensors based on the flexible dipicolylamine and quinoline. *Inorg Chim Acta* 2013;394:542–51.
 - Li P, Zhou X, Huang R, Yang L, Tang X, Dou W, et al. A highly fluorescent chemosensor for Zn^{2+} and the recognition research on distinguishing Zn^{2+} from Cd^{2+} . *Dalton Trans* 2014;43:706;
 - Liu Z, Zhang C, Chen Y, Qian F, Bai Y, He W, et al. In vivo ratiometric Zn^{2+} imaging in sebrafish larvae using a new visible light excitable fluorescent sensor. *Chem Commun* 2014;50:1253;
 - Mikata Y, Yamashita A, Kawata K, Konno H, Itami S, Yasuda K, et al. Methoxyquinoline-diethylenetriamine conjugated as a fluorescent zinc sensor. *Dalton Trans* 2011;40:4976.
- Recent examples a) Zhang C, Liu Z, Li Y, He W, Gao X, Guo Z. *In vitro* and *in vivo* imaging application of a 1,8-naphthalimide-derived Zn^{2+} fluorescent sensor with nuclear envelope penetrability. *Chem Commun* 2013;49:11430–2;
 - Meeusen J, Tomasiewicz H, Nowakowski A, Petering DH. TSQ (6-methoxy-8-*p*-toluenesulfonamido-quinoline), a common fluorescent sensor for cellular zinc, images zinc proteins. *Inorg Chem* 2011;50:7563–73;
 - Yang XB, Yang BX, Ge JF, Xu YJ, Xu QF, Liang J, et al. Benzo[a]phenoxazinanium-based red-emitting chemosensor for zinc ions in biological media. *Org Lett* 2011;13:2710;
 - Das P, Bhattacharya S, Mishra S, Das A. Zn(II) and Cd(II)-based complexes for probing the enzymatic hydrolysis of $\text{Na}_4\text{P}_2\text{O}_7$ by alkaline phosphatase in physiological conditions. *Chem Commun* 2011;47:8118–20;
 - Lee AE, Grace MR, Meyer AG, Tuck KL. Fluorescent Zn^{2+} chemosensors, functional in aqueous solution under environmentally relevant conditions. *Tetrahedron Lett* 2010;51:1161–5;
 - Liu Z, Zhang C, Li Y, Wu Z, Qian F, Yang X, et al. A Zn^{2+} fluorescent sensor derived from 2-(pyridine-2-yl)benzimidazole with ratiometric sensing potential. *Org Lett* 2009;11:795–8;
 - Kwon KE, Lee S, You Y, Baek KH, Ohkubo K, Cho J, et al. Fluorescent zinc sensor with minimized proton-induced interferences: photophysical mechanism for fluorescence response and detection of endogenous free zinc ions. *Inorg Chem* 2012;51:8760–74;
 - Lee HG, Lee JH, Jang SP, Park HM, Kim SJ, Kim Y, et al. Zinc selective chemosensor based on pyridyl-amide fluorescence. *Tetrahedron* 2011;67:8073–8;
 - Kuang GC, Allen JR, Baird MA, Nguyen BT, Zhang L, Morgan TJ, et al. Balance between fluorescence enhancement and association affinity in fluorescent heteroditopic indicators for imaging zinc ion in living cells. *Inorg Chem* 2011;50:10493–504;
 - Zhang JF, Kim S, Han JH, Lee SJ, Pradhan T, Cao QY, et al. Pyrophosphate-selective fluorescent chemosensor based on 1,8-naphthalimide-dpa-Zn(II) complex and its application for cell imaging. *Org Lett* 2011;13:5294–7;
 - Xue L, Li G, Yu C, Jiang H. A ratiometric and targetable fluorescent sensor for quantification of mitochondrial zinc ions. *Chem Eur J* 2012;18:1050–4;
 - Wang X, Liu Z, Qian F, He W. A benzimidazole-based highly selective and low-background fluorescent sensor for Zn^{2+} . *Inorg Chem Commun* 2012;15:176–9;
 - Meng X, Wang S, Li Y, Zhu M, Guo Q. 6-substituted quinoline-based ratiometric two-photon fluorescent probes for biological Zn^{2+} detection. *Chem Commun* 2012;48:4196–8;
 - Xu Z, Kim GH, Han SJ, Jou MJ, Lee C, Shin I, et al. An NBD-based colorimetric and fluorescent chemosensor for Zn^{2+} and its use for detection of intracellular zinc ions. *Tetrahedron* 2009;65:2307–12;
 - Hanaoka K, Muramatsu Y, Urano Y, Terai T, Nagano T. Design and synthesis of a highly sensitive off-on fluorescent chemosensor for zinc ions utilizing internal charge transfer. *Chem Eur J* 2010;16:568;
 - Atilgan S, Ozdemir T, Akkaya EU. A sensitive and selective ratiometric near IR fluorescent probe for zinc ions based on the distyryl-bodipy fluorophore. *Org Lett* 2008;10:4065;
 - Jiang W, Fu Q, Fan H, Wang W. A NBD fluorophore-based sensitive and selective fluorescent probe for zinc ion. *Chem Commun* 2008:259–61;
 - Qian F, Zhang C, Zhang Y, He W, Gao X, Hu P, et al. Visible light excitable Zn^{2+} fluorescent sensor derived from an intramolecular charge transfer fluorophore and its *in vitro* and *in vivo* application. *J Am Chem Soc* 2009;131:1460–8.
 - Wang HH, Gan Q, Wang XJ, Xue L, Liu SH, Jiang H. A water-soluble, small molecular fluorescent sensor with femtomolar sensitivity for zinc ion. *Org Lett* 2007;9:4995–8;
 - Xue L, Liu C, Jiang H. A ratiometric fluorescent sensor with a large Stokes shift for imaging zinc ions in living cells. *Chem Commun* 2009:1061–3;
 - Chen XY, Shi J, Li YM, Wang FL, Wu X, Guo QX, et al. Two-photon fluorescent probes of biological Zn(II) derived from 7-hydroxyquinoline. *Org Lett* 2009;11:4426–9;
 - Xue L, Liu Q, Jiang H. Ratiometric Zn^{2+} fluorescent sensor and new approach for sensing Cd^{2+} by ratiometric displacement. *Org Lett* 2009;11:3454–7;
 - Tomat E, Lippard SJ. Ratiometric and intensity-based zinc sensors built on rhodol and rhodamine platforms. *Inorg Chem* 2010;49:9113–5;

- f) Mikata Y, Yamashita A, Kawata K, Konno H, Itami S, Yasuda K, et al. Methoxy-substituted isoTQEN family for enhanced fluorescence response toward zinc ion. *Dalton Trans* 2011;40:4059–66.
- [8] Berkel PM, Driessen WL, Hämäläinen R, Reedijk J, Turpeinen U. Coordination compounds of the chelating tridentate pyrazole-containing ligand bis[2-(3,5-dimethyl-1-pyrazolyl)ethyl]amine (ddaH). *Inorg Chem* 1994;33:5920–6.
- [9] a) Lian B, Thomas CM, Casagrande OL, Lehmann CW, Roisnel T, Carpentier JF. Aluminum and zinc complexes based on a amino-bis(pyrazolyl) ligand: synthesis, structures and use in MMA and lactide polymerization. *Inorg Chem* 2007;46:328–40;
b) Castellano MdC, Pons J, García-Antón J, Solans X, Font-Bardía M, Ros J. Coordination compounds of Zn(II) with several bidentate-*NN* and tridentate-*NNN* nitrogen donor ligands. *Inorg Chim Acta* 2008;361:2923–8;
c) Massoud SS, Louka FR, Obaid YK, Vicente R, Ribas J, Fischer RC, et al. Metal ions directing the geometry and nuclearity of azido-metal(II) complexes derived from bis(2-(3,5-dimethyl-1*H*-pyrazol-1-yl)ethyl)amine. *Dalton Trans* 2013;42:3968–78;
d) Alam R, Mistri T, Mondal P, Das D, Mandal SK, Khuda-Bukhsh AR, et al. A novel copper(II) complex as a nitric oxide turn-on fluorosensor: intracellular applications and DFT calculation. *Dalton Trans* 2014;43:2566–76.
- [10] Rastogi SK, Pal P, Aston DE, Bitterwolf TE, Branen AL. 8-aminoquinoline functionalized silica nanoparticles: a fluorescent nanosensor for detection of divalent zinc in aqueous and in yeast cell suspension. *ACS Appl Mater Interfaces* 2011;3:1731–9.
- [11] Mistri T, Alam R, Dolai M, Mandal SK, Khuda-Bukhsh AR, Ali MA. 7-nitrobenz-2-oxa-1,3-diazole based highly sensitive and selective turn-on chemosensor for copper(II) ion with intracellular application without cytotoxicity. *Org Biomol Chem* 2013;11:1563–9.